Task-Consistent Obstacle Avoidance and Motion Behavior for Mobile Manipulation

Oliver Brock   Oussama Khatib   Sriram Viji
Robotics Laboratory, Department of Computer Science
Stanford University, Stanford, California 94305
email: {oli, khatib}@cs.stanford.edu   sviji@stanford.edu

Abstract

Applications in mobile manipulation require sophisticated motion execution skills to address issues like redundancy resolution, reactive obstacle avoidance, and transitioning between different motion behaviors. The elastic strip framework is an approach to reactive motion generation providing an integrated solution to these problems. Novel techniques within the elastic strip framework are presented, allowing task-consistent obstacle avoidance and task-consistent motion behavior. General transition criteria and methods are presented, permitting the suspension and resumption of task execution to ensure other desired motion behavior, such as obstacle avoidance. Task execution has to be suspended when kinematic constraints or changes in the environment render task-consistent motion behavior infeasible. Task execution is resumed as soon as it is consistent with other desired motion behavior.

1   Introduction

Mobile manipulation poses new challenges to motion planning and control algorithms. Applications with more sophisticated task requirements call for the integration of different behaviors during a motion. The motion of robots in populated environments, for example, has to combine task execution and obstacle avoidance to react to unforeseen changes in dynamic environments. For redundant mechanisms those degrees of freedom not being used to accomplish the task can be used to generate additional desired behavior. A motion generation framework suitable for mobile manipulation has to address these diverse motion generation requirements.

When a manipulator arm is mounted on a mobile base, the resulting robotic system is oftentimes redundant with respect to the task of orienting and positioning the end-effector. Various schemes for redundancy resolution have been proposed [5, 7, 11]. These approaches provide a framework for the integration of

end-effector motion with motion only affecting redundant degrees of freedom. The approach presented in this paper relies on the operational space formulation [5], using the dynamically consistent force/torque relationship [6] to control the end-effector position and orientation and the redundant degrees of freedom of a mechanism independently.

Several approaches for the integration of different aspects of motion for robotic systems have been proposed. Given a trajectory of the end-effector, the base of a vehicle/arm system can be positioned automatically to keep the end-effector in the center of its work space [13]. Executing a motion with a mobile manipulator, the trajectory of the arm can be modified to reactively avoid obstacles without affecting the motion of the base [9, 12]. A potential field-based approach combines a task potential, causing the end-effector to follow a given trajectory, a coordination potential, resulting in base motion to center the end-effector in its work space, and an obstacle avoidance potential to generate motion for a mobile manipulator [10]. Another approach allows to control the balance of a humanoid robot, while choosing an overall posture that maximizes the work space of the arms [3].

The elastic strip framework [2] is a general approach for integration of behavior during reactive motion execution. It allows the combination of task execution, obstacle avoidance, and posture control [1]. During task-constrained motion execution for mobile manipulation, however, it may become necessary to transition between different motion behaviors: Assume a mobile manipulator is performing a task while reactively avoiding obstacles using redundant degrees of freedom. As the robot reaches the limit of its work space, the range of motion resulting from only redundant degrees of freedom is significantly reduced. Consequently, the task might have to be suspended to ensure collision avoidance. It can be resumed after the obstacle has been cleared by the mobile manipulator. This paper presents task-consistent obstacle avoidance behavior in the elastic strip framework and an approach for tran-

sitioning between different motion behaviors.

2   Elastic Strip Framework

The elastic strip framework [2] allows real-time path modification for robots with many degrees of freedom in dynamic environments. The representation of an initial path, called *candidate path*, is augmented by a set of paths homotopic to it. During the execution of the motion a new candidate path is chosen from this set multiple times per second, taking into account the most current information about the environment, thus allowing the integration of task behavior, obstacle avoidance, and posture control.

2.1   Sets of Homotopic Paths

Let $\mathcal{P}_c$ be a path generated by a planner. This path represents a collision free motion accomplishing a given task; we will call it *candidate path*. Furthermore, let $V_\mathcal{P}^\mathcal{R}$ be the work space volume swept by robot $\mathcal{R}$ along trajectory $\mathcal{P}$.[1] This work space volume can be seen as an alternative representation of the one-dimensional curve $\mathcal{P}$ in configuration space. Let $V_\mathcal{P}^\delta$ be defined as

$$V_\mathcal{P}^\delta := (V_\mathcal{P} \oplus b_\delta)\backslash V_\mathcal{O},$$

where $\oplus$ is the Minkowski sum operator, b_δ designates a ball of radius δ centered around the origin, and $V_\mathcal{O}$ is the work space volume occupied by obstacles. $V_\mathcal{P}^\delta$ corresponds to $V_\mathcal{P}$ grown by δ in all directions, excluding the work space volume occupied by obstacles. Assuming that the robot is not in contact with obstacles along the entire path, it is obvious that there exists a path $\mathcal{P}' \neq \mathcal{P}$ homotopic to $\mathcal{P}$ and obtained from $\mathcal{P}$ by a slight modification, such that $V_{\mathcal{P}'} \subset V_\mathcal{P}^\delta$. Therefore, $V_\mathcal{P}^\delta$ can be seen as an implicit representation of paths homotopic to the candidate path $\mathcal{P}_c$.

In the elastic strip framework a work space volume of free space surrounding $V_{\mathcal{P}_c}$ is computed. Since, depending on the method of computation, it might not be identical to $V_\mathcal{P}^\delta$ we will denote it by $\mathcal{T}_{\mathcal{P}_c}$ and call it *elastic tunnel* of free space. This tunnel represents a work space volume implicitly describing a set of paths $P(\mathcal{T}_{\mathcal{P}_c})$ homotopic to $\mathcal{P}_c$:

$$P(\mathcal{T}_{\mathcal{P}_c}) := \{\ \mathcal{P}\ |\ V_\mathcal{P} \subset \mathcal{T}_{\mathcal{P}_c}\ \text{and}\ \ \mathcal{P} \simeq \mathcal{P}_c\ \},$$

where $\simeq$ denotes the homotopy relation between two paths. Given a candidate path $\mathcal{P}_c$, a corresponding tunnel $\mathcal{T}_{\mathcal{P}_c}$ can be easily computed [1] using distance computations in the work space. An elastic strip $\mathcal{S}$ is

a tuple consisting of a candidate path and the corresponding elastic tunnel; it is defined as $\mathcal{S} := (\mathcal{P}_c, \mathcal{T}_{\mathcal{P}_c})$

An example of an elastic tunnel, given a particular scheme of free space computation, is shown in Figure 1. Three configurations of the Stanford Mobile Manipulator along a given path are displayed. The overlapping, transparent spheres indicate the computed free space. The union of those spheres represents the elastic tunnel.
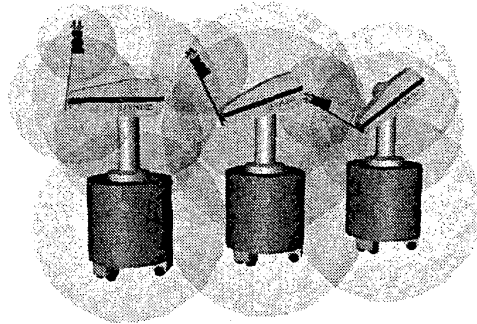

Figure 1: Three configurations along a trajectory are shown. The transparent spheres indicate an approximation of local free space (obstacles are not shown). The union of their volume constitutes an elastic tunnel of free space.

2.2   Selection of a Path

Given an elastic strip $\mathcal{S}$, an algorithm is required to efficiently select a new candidate path $\mathcal{P}'_c$ from the elastic tunnel. Using a potential field-based control algorithm real-time performance can be achieved. Rather than exploring the entire configuration space, it maps proximity information from the environment into the configuration space, using the kinematic structure of the manipulator. The elastic strip framework differs from other reactive approaches in that potential fields are applied to a discretized representation of the entire trajectory and not only to a particular configuration of the robot.

The trajectory is exposed to forces, acting in the work space, incrementally modifying the candidate path to yield a new one. The forces are derived from three potential functions, the external, internal, and posture potential, $V_{external}, V_{internal}$, and $V_{posture}$, respectively. The external, repulsive potential $V_{external}$ is defined as a function of proximity to obstacles. Minimizing this potential effectively maximizes the clearance of the path to obstacles in the environment. For a point p on a configuration of the robot along the

---

[1]For simplicity we will drop the exponent $\mathcal{R}$ in the remainder of this paper. Unless noted, variables refer to the robot $\mathcal{R}$.

trajectory the external potential is defined as

$$V_{external}(p) = \begin{cases} \frac{1}{2}k_r(d_0 - d(p))^2 & \text{if } d(p) < d_0 \\ 0 & \text{otherwise} \end{cases},$$

where $d(p)$ is the distance from p to the closest obstacle, d_0 defines the region of influence around obstacles, and k_r is the repulsion gain. The force resulting from this potential that acts on point p is given by:

$$F_p^{ext} = -\nabla V_{external} = k_r(d_0 - d(p))\frac{\vec{d}}{\|\vec{d}\|},$$

where $\vec{d}$ is the vector between p and the closest point on the obstacle. Intuitively, the repulsive potential pushes the trajectory away from obstacles, if it is inside their influence region. Using the external forces to select a new candidate path maintains the global properties of the path and local minima can be avoided.

The external potential alone would suffice in most cases to select a new candidate path, as repulsive forces keep the trajectory in free space. If an obstacle deforming a path would recede, however, the path would never shorten. Virtual springs attached to control points on consecutive configurations of the robot along the elastic strip can achieve this effect. Let p_j^i be the position vector of the control point attached to the j-th joint of the robot in configuration q_i. The internal contraction force acting at control point j of the ith configuration, caused by the virtual spring connecting it to the $i-1$st and the $i+1$st configuration along the path $\mathcal{P}$, is defined as:

$$F_{i,j}^{int} = k_c \left(\frac{d_j^{i-1}}{d_j^{i-1} + d_j^i}(p_j^{i+1} - p_j^{i-1}) - (p_j^i - p_j^{i-1}) \right),$$

where d_j^i is the distance $\|p_j^i - p_j^{i+1}\|$ in the initial, unmodified trajectory and k_c is a constant determining the contraction gain of the elastic strip. This approach differs from the virtual spring method [8] in that springs do not represent a link but connect the same link in different virtual configurations.

Using the external and internal forces, the elastic strip behaves like a strip of rubber. Obstacles cause it to deform, and as obstacles recede it assumes its previous shape. The forces are mapped to joint displacements using a kinematic model of the manipulator. This effectively replaces configuration space exploration with a directed search, guided by work space forces. The computation is virtually independent of the dimensionality of the configuration space [1].

In case of redundant manipulators, a third potential is introduced. The potential $V_{posture}$ can be used to define a preferred posture for the robot in absence of other constraints. This allows, for example, to maintain the most stable or energy-conserving position when manipulating a heavy load. Based on the dynamically consistent decoupling of task execution and nullspace motion [5], the motion resulting from these three potentials can be combined with the motion required for task execution. Motion in the nullspace of the task is used to avoid obstacles, shorten the trajectory, and achieve a desired posture in a task-consistent manner. The details of this integration are described in the next section.

3 Task-Consistency for Obstacle Avoidance

The equations of motion of a non-redundant manipulator in operational space are given by

$$\Lambda(\mathbf{x})\ddot{\mathbf{x}} + \mu(\mathbf{x}, \dot{\mathbf{x}}) + \mathbf{p}(\mathbf{x}) = \mathbf{F},$$

where $\mathbf{x}$ is the vector of operational space coordinates, $\Lambda(\mathbf{x})$ is the operational space mass matrix, $\mu(\mathbf{x}, \dot{\mathbf{x}})$ is the vector of centrifugal and Coriolis forces, and $\mathbf{p}(\mathbf{x})$ is the vector of gravity forces [5]. The vector of joint torques Γ required to achieve forces and moments $\mathbf{F}$ at the end-effector can be computed using

$$\Gamma = J^T(\mathbf{q})\,\mathbf{F}. \tag{1}$$

Using equation 1, manipulators can be controlled in operational space.

For redundant manipulators the relationship between generalized operational forces and joint torques from equation 1 becomes incomplete. The Jacobian associated with redundant manipulators has a nullspace. Torques mapped into the nullspace of the Jacobian will not affect the end-effector motion. For redundant manipulators the relationship between operational forces and joint torques is given by:

$$\Gamma = J^T(\mathbf{q})\,\mathbf{F} + \left[I - J^T(\mathbf{q})\,\bar{J}^T(\mathbf{q})\right]\Gamma_0, \tag{2}$$

where I is the identity matrix, $\bar{J}$ is the dynamically consistent inverse [4], A is the joint space mass matrix, and Γ_0 is a vector of joint torques. The control of a redundant manipulator with equation 2 effectively decomposes joint torques into those acting at the end-effector ($J^T(\mathbf{q})\,\mathbf{F}$) and those only affecting interior motion of the manipulator ($\left[I - J^T(\mathbf{q})\,\bar{J}^T(\mathbf{q})\right]\Gamma_0$). Using this decomposition the integration of various motion behaviors is achieved in the elastic strip framework [1]. The vector of forces and moments $\mathbf{F} = -\nabla V_{task}$ is derived from the task potential V_{task}. The torques resulting from forces caused by obstacles ($V_{external}$), internal forces ($V_{internal}$), and

posture constraints ($V_{posture}$) are mapped into the nullspace, thereby not affecting task execution. The posture potential can be defined to accomplish arbitrary nullspace behavior, such as centering the manipulator arm in its work space, or maintaining the balance of a humanoid robot. The different potentials acting in the nullspace can be prioritized using a simple weighting scheme for the resulting torques.

4 Transitioning Behavior

The previous sections introduced the elastic strip framework and showed how the operational space formulation [5] can be used to integrate various aspects of motion behavior during reactive motion execution. This approach can fail, however, when the torques resulting from mapping Γ_0 into the nullspace (see equation 2) yield insufficient motion to accomplish the desired behavior. If that behavior has higher priority than task execution, as it would be the case for obstacle avoidance, task execution has to be suspended. The behavior previously executed in the nullspace can then be executed using all degrees of freedom of the robot. When possible, task execution is resumed. This section introduces criteria for determining when such a transition is required and methods for performing such a transition.

4.1 Transition Criteria

Let $\mathcal{N}^T(J(\mathbf{q})) := \left[I - J^T(\mathbf{q}) \, \bar{J}^T(\mathbf{q}) \right]$ be the dynamically consistent nullspace mapping of the Jacobian $J(\mathbf{q})$ associated with the task. The coefficient

$$c := \frac{\| \mathcal{N}^T(J(\mathbf{q})) \, \Gamma_0 \|}{\| \Gamma_0 \|}$$

corresponds to the ratio of the magnitude of the torque vector Γ_0 mapped into that nullspace to its unmapped magnitude. This coefficient is an indication of how well the behavior represented by Γ_0 can be performed inside the nullspace of the task. We experimentally determine a value c_s at which it is desirable to suspend task execution in favor of the behavior previously mapped into the nullspace. Once the coefficient c assumes a value $c < c_s$, a transition is initiated. During this transition task behavior is gradually suspended and previous nullspace behavior is performed using all degrees of freedom of the manipulator. The transition itself is described in the next section.

The reverse transition to resume task behavior is initiated when the magnitude of a vector $\mathbf{F}_r$, representing the forces and moments applied at the end-effector to resume the task, becomes smaller than a threshold

ϵ, $\|\mathbf{F}_r\| \leq \epsilon$, and simultaneously $c > c_r$, where c_r is a threshold of the coefficient c for resuming the task. This condition is an indication that the task can be executed while realizing the behavior entirely in the nullspace. The value for c_r is chosen so that $c_r > c_s$; this deadband between c_s and c_r avoids unnecessary transitions.

4.2 Transition Methods

The transition to suspend the task execution is performed based on the coefficient c and a desired duration t_s for the transition. Transitions are characterized by a transition variable $\alpha \in [0, 1]$. When suspending the task, $\alpha_{suspend}$ is given by

$$\alpha_{suspend} := \left\{ \begin{array}{ll} \min(\frac{c}{c_0}, 1 - \frac{t-t_0}{t_s}) & \text{if } t - t_0 < t_s \\ 0 & \text{otherwise} \end{array} \right. ,$$

where t is the current time t_0 is the time at which the transition was initiated. The time-based component allows a smooth transition under normal circumstances, whereas considering c permits to react more rapidly to extreme situations, in which the mapping into the nullspace yields only very minimal torques.

The transition to resume the task is performed entirely based on the desired duration t_r; the transition variable α_{resume} is defined as

$$\alpha_{resume} := \left\{ \begin{array}{ll} \frac{t-t_0}{t_r} & \text{if } t - t_0 < t_r \\ 1 & \text{otherwise} \end{array} \right. .$$

The parameters t_s and t_r can be chosen based upon the acceleration capabilities of the manipulator and the expected rate of change in the environment. They affect the appearance of the resulting overall motion.

The motion of the manipulator is generated using the equation

$$\begin{array}{rl} \Gamma = & f(\alpha) \quad J^T(\mathbf{q}) \, \mathbf{F} \, + \\ & f(\alpha) \quad [I - J^T(\mathbf{q}) \, \bar{J}^T(\mathbf{q})] \, \Gamma_0 \, + , \\ & f(\bar{\alpha}) \quad \Gamma_0 \end{array}$$

where $\bar{\alpha} := (1 - \alpha)$ is defined as the complement of α ($\alpha_{suspend}$ or α_{resume} depending on the transition), and $f(\cdot)$ is the transition function, determining the rate of change during the transition. The simplest choice for $f(\cdot)$ is the identity function, in which case the transition variable α will generate a linear transition over time, unless the coefficient c drops too quickly. Smoother transitions can be generated using a sigmoidal function $f(x) = \frac{1}{1+e^{-x}}$, translated and scaled to the interval $[0, 1]$. The condition of $f(\alpha) + f(\bar{\alpha}) = 1$ for all $\alpha \in [0, 1]$ is not necessary for a particular choice of f; it is desirable, however, to maintain this property at the end points of that interval.
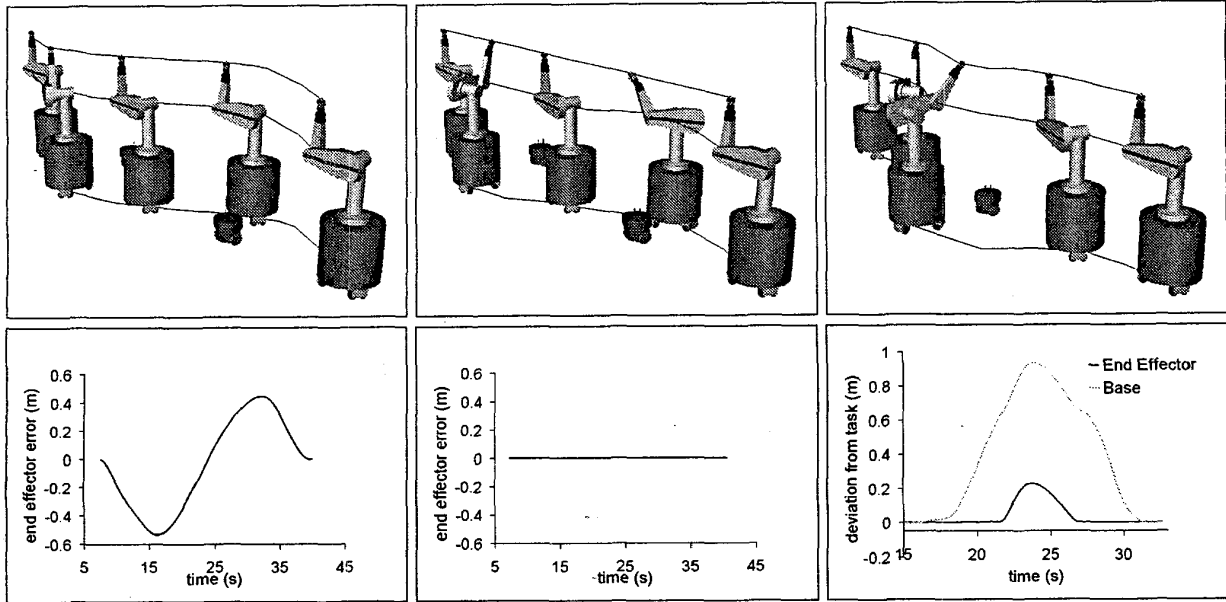
Figure 2: Top images show from left to right: real-time path modification without task consistency, with task consistency, and transitioning between task-consistent and non task-consistent behavior. Lines indicate the trajectory of the base, elbow, and end-effector. The graphs below the images show end-effector error and base deviation from the task for the respective experiment. Pure path modification will lead to large end-effector errors. Task-consistent path modification allows the combination of task execution and obstacle avoidance. The experiment on the right shows the base trajectory and end-effector motion when the task has to be suspended.

5 Experimental Results

The proposed algorithms were implemented and tested on the Stanford Mobile Manipulator, a holonomic mobile base combined with a PUMA 560 manipulator arm. The task in the experiments presented in Figures 2 and 3 requires the end-effector to follow a straight-line trajectory. The redundant degrees of freedom are used to avoid obstacles. Without task consistency the base and the end-effector deviate significantly from the task. When obstacle avoidance is performed in a task-consistent manner, the end-effector deviates very little from the task. During experiments with the real robot an error of $3.5mm$ is not exceeded (see graphs and caption of Figure 2). The base, however, performs significant motion to avoid obstacles. In a different experiment, shown in the rightmost images in Figure 2, obstacle motion renders task-consistent obstacle avoidance impossible and the task is suspended. Initally, task-consistency results in very little end-effector error, despite significant base motion. During the time interval between $t = 22s$ and $t = 27s$, however, obstacle avoidance of the base renders task execution infeasible and an error of up to $22cm$ is introduced. After the robot passes the obstacle, the task is resumed in a

smooth motion.

During the experiments the transition time parameters were $t_s = t_r = 1s$. For the transition coefficients the following values were used: $c_s = 0.2$ and $c_r = 0.3$. For experiments on the real robot a SICK laser range finder was used to detect obstacles. Figure 3 shows snapshots of the motion generated for the Stanford Mobile Manipulator as an obstacle moves into its path. The obstacle is avoided using task-consistent, real-time path modification. Despite large base motion the end-effector performs a straight-line trajectory.

6 Conclusion

The elastic strip framework is a versatile approach to reactive motion generation for robots with many degrees of freedom in dynamic environments. By representing a set of homotopic paths implicitly as a work space volume, called the elastic tunnel, and incrementally modifying the path within that tunnel, real-time motion modification can be achieved. Since elastic strips allow the integration of various motion behaviors, such as task execution, obstacle avoidance, and posture control, it is particularly well suited for mo-
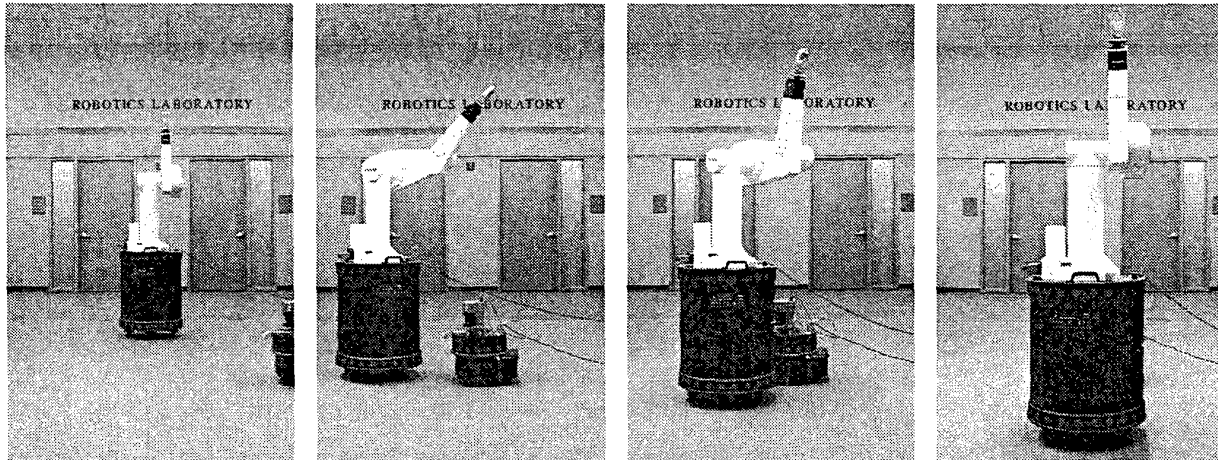
Figure 3: Task-consistent real-time path modification using the nine degree-of-freedom Stanford Mobile Manipulator: despite the base changing its trajectory to avoid the moving obstacle, the end-effector performs the task of following a straight-line trajectory. During the experiment, the obstacle is perceived using a laser range finder.

bile manipulation. Task requirements, kinematic constraints of the robot, or obstacles in the environment, however, can render such an integration temporarily impossible. The elastic strip framework provides criteria to detect this situation and allows for a simple transition between different motion behaviors to ensure the execution of the highest-priority behavior. Once possible, the original behavior is restored. Experimental results on the Stanford Mobile Manipulator were presented, demonstrating the effectiveness of the approach.

Acknowledgments

References

[1] O. Brock. *Generating Robot Motion: The Integration of Planning and Execution*. PhD thesis, Stanford University, Stanford University, USA, 2000.

[2] O. Brock and O. Khatib. Real-time replanning in high-dimensional configuration spaces using sets of homotopic paths. In *Proc. of the Intl. Conf. on Robotics and Automation*, volume 1, pages 550–555, San Francisco, USA, 2000.

[3] K. Inoue, H. Yoshida, T. Arai, and Y. Mae. Moblie manipulation of humanoids -- real-time control based on manipulability and stability. In *Proc. of the Intl. Conf. on Robotics and Automation*, San Francisco, USA, 2000.

[4] O. Khatib. *Command Dynamique dans l'Espace Opérationel des Robots Manipulateurs en Présence d'Obstacle*. PhD thesis, Ecole Nationale Supérieur de l'Aéronautic et de l'Espace, Toulouse, France, 1980.

[5] O. Khatib. A unified approach to motion and force control of robot manipulators: The operational space formulation. *Intl. Journal of Robotics and Automation*, 3(1):43–53, 1987.

[6] O. Khatib. Inertial properties in robotics manipulation: An object-level framework. *Intl. Journal of Robotics Research*, 14(1):19–36, 1995.

[7] O. Khatib, Kazu Yokoi, O. Brock, Kyong-Sok Chang, and Arancha Casal. Robots in human environments: Basic autonomous capabilities. *Intl. Journal of Robotics Research*, 18(7):684–696, 1999.

[8] A. McLean and S. Cameron. The virtual springs method: Path planning and collision avoidance for redundant manipulators. *Intl. Journal of Robotics Research*, 15(4):300–319, 1996.

[9] U. M. Nassal. Motion coordination and reactive control of autonomous multi-manipulator systems. *Journal of Robotic Systems*, 13(11):737–754, 1996.

[10] P. Ögren, M. Egerstedt, and X. Hu. Reactive mobile manipulation using dyanmic trajectory tracking. In *Proc. of the Intl. Conf. on Robotics and Automation*, pages 3473–3478, San Francicso, USA, 2000.

[11] H. Seraji. An on-line approach to coordinated mobility and manipulation. In *Proc. of the Intl. Conf. on Robotics and Automation*, volume 1, pages 28–35, 1993.

[12] Y. Yamamoto and X.Yun. Coordinated obstacle avoidance of a mobile manipulator. In *Proc. of the Intl. Conf. on Robotics and Automation*, volume 3, pages 2255–2260, 1995.

[13] Y. Yamamoto and X. Yun. Coordinating locomotion and manipulation of a mobile manipulator. *IEEE Trans. on Automatic Control*, 39(6):1326–1332, 1994.